Zeeman Effect Observations in Class I Methanol Masers toward Supernova Remnants

Justin Potvin

Spring Quarter 2017

Thesis submitted in partial completion of Senior Honors Capstone requirements for the DePaul University Honors Program

Thesis Director: Dr. A. P. Sarma, Physics Department

Faculty Reader: Dr. J. Pando, Physics Department

Table of Contents:

Abstract

This thesis presents observations of 36 GHz Class I methanol masers taken with the Karl G. Jansky Very Large Array (VLA) with the aim of detecting the Zeeman Effect. The Zeeman effect is the most direct way to measure magnetic fields in astronomical environments. Since magnetic fields are known to play an important role in star formation, it is important to measure them in as many environments as possible. In particular, supernova remnants provide material that enriches a subsequent generation of stars. We targeted two Class I methanol maser sources (GCMM1 and GCMM4) in the supernova remnant Sagittarius A toward the Galactic Center. Each source was observed for three hours. The observed spectral profiles of the masers are complex, with several components blended in velocity. Four Gaussian components were fitted to each of the two maser sources. The derivatives of these profiles were fitted to the observed Stokes *V* profile, a standard way to measure the Zeeman effect. In only one case was the Stokes *V* maser profile prominent enough to reveal a 2.6-sigma hint of a magnetic field of zB_{los} = 14.56 +/- 5.60 Hz; we have chosen to express our results in terms of zB_{los} since the Zeeman splitting factor (z) for 36 GHz methanol masers has never been measured. Either the magnetic field in both sources is largely in the plane of the sky so that its line of sight component is small, or the field reverses on very small scales so that it cancels out in summing over the four components. We believe that these spectra would reveal significant magnetic fields if they could be spatially and spectrally resolved. We also believe that future observations would be successful in detecting magnetic fields if maser sources exist that have simpler profiles, or if environments exist in which the field is overwhelmingly large in one component.

Acknowledgments

I would like to thank Dr. Sarma for the opportunity to work with him on this as well as many previous research projects. With his guidance and support I have learned a great deal throughout my time at DePaul University. I want to thank my NRAO advisor who oversaw my research, Dr. Momjian. I want to also thank Dr. Pando for being my Thesis Reader on this project and for the feedback he has provided. A final thank you to the Honors Program at DePaul University for fostering a diverse curriculum and a tight community of dedicated students.

1. Introduction

Throughout human history, people have been entranced by the stars that shine brightly in the darkness of the night. The brightest stars we see in the sky are high mass stars in our Galaxy (stars with masses eight times that of the Sun, or greater). Such stars usually end their life cycles in supernovae (so called because, historically, they appeared suddenly as bright stars in a hitherto empty region of the sky and then faded over time). Material left over from the supernova forms a structure known as a supernova remnant, an example of which can be seen in Figure 1.

Figure 1. Image of Cassiopeia A, a type II supernova remnant located within the constellation of Cassiopeia. Type II supernova remnants are the remains after a massive star has rapidly collapsed and exploded (Williams).

Since elements above iron in the Periodic Table are formed in supernovae, supernova remnants are repositories of material that enrich the next generation of stars. Stars constitute much of the visible material in the sky and are prominent members of the evening sky and so there has long been interest in understanding how they form. Despite great advancements in our understanding of star formation, however, there is still much to learn. One thing we do know is that magnetic fields have some involvement with the formation. Therefore, one would like to measure magnetic fields in as many regions in space as possible, especially within regions where high mass stars form. The most direct way to measure magnetic fields in space is by observing the Zeeman effect. The Zeeman effect is responsible for splitting energy levels in atoms or molecules when these atoms or molecules are placed in a magnetic field. Therefore, the Zeeman effect would cause multiple spectral lines to appear where one would observe only one spectral line, for example, in the absence of a magnetic field. In 2009, Sarma and Momjian discovered the Zeeman effect in the spectrum of a Class I methanol maser toward the star forming region M8E. Masers are like lasers, except that they occur in the microwave region of the electromagnetic spectrum. Maser emission is produced when some process causes molecules (or atoms) to gather in an excited energy state, a condition known as population inversion, and some stimulant causes all these molecules or atoms to cascade down to a lower energy state. In Class I methanol masers, population inversion is caused by collisions among molecules. Since supernovae cause ejected material from the star to collide violently with ambient material, we would expect Class I methanol masers to occur in supernova remnants. Indeed, Sjouwerman and collaborators (2010) discovered ten Class I methanol masers in a supernova remnant known as Sagittarius A that is located toward the center of our Galaxy. Measurement of the Zeeman effect in these masers would tell us about the magnetic field in these regions, and how they might affect the formation of a subsequent generation of stars.

Section 2 describes the observations reported in this thesis and also contains an overview of the most important steps in the data reduction procedures necessary for a scientific investigation of the observed data. Section 3 presents the results of the observations. These results are discussed and analyzed in Section 4, and conclusions from this work are summarized in Section 5.

2. Observation and Data Reduction

The masers studied in this thesis are located in a supernova remnant toward the Galactic Center. Observations of this supernova remnant were taken using the Very Large Array (VLA)[1] radio telescope array in New Mexico. The observations were planned and made by Dr. Sarma with assistance from his collaborator, Dr. Emmanuel Momjian (NRAO), prior to the work reported in this thesis. Table 1 lists the observing parameters and other relevant data for these observations. Two of the strongest masers in the supernova remnant (GCMM1 and GCMM4) were each observed for three hours with the VLA. The initial activity for the project reported in this thesis was to import all of the observed VLA data using the Astronomical Imaging Processing Software (AIPS) data reduction package provided by the NRAO. Once this was accomplished the logs written by the VLA operator were checked for any antennas that had errors occur with them. Following standard procedure, the corresponding data were then located within AIPS and erased so as to not skew our results. The next step was to calibrate the data to ensure that all observed sources had the correct intensities. Three standard sources, J1745-2900, J1733-1304, and 1331+305 (3C286), were used in this initial calibration step. The peak spectral channel for every maser was then separated and self-calibrated. Self-calibration is an iterative process in which an initial image of the observed region is used as a reference to improve the final image. The results of this self-calibration were then applied to the full spectral line dataset. Finally, images of the observed masers in the supernova remnant were prepared using the AIPS software. Measurement of the Zeeman effect requires images to be prepared in the Stokes *I* and *V* parameters. Images in the Stokes *I* parameter are of the total intensity of the maser as we scan in frequency across different spectral channels. Images in the Stokes *V* parameter are of the difference between right and left circularly polarized signals from the masers. Circular

[1] The Very Large Array (VLA) is managed by the National Radio Astronomy Observatory (NRAO), a facility of the National Science Foundation operated under cooperative agreement by Associated Universities, Inc.

polarization of an electromagnetic wave is when the electric field vector of the wave rotates in a circle. The Stokes *I* and *V* profiles were then used to search for the Zeeman effect, as described in the next section.

Table 1. Observational Parameters for VLA observations

Source	GCMM1	GCMM4
Observation Date	08/18/2012	07/31/2012
Right Ascension of field center[a]	17 45 50.086	17 45 37.667
Declination of field center [a]	-28 59 40.65	-29 03 45.41
VLA Configuration	B	
Total Bandwidth (MHz)	1.000	
Number of channels	256	
Channel spacing (kHz)	3.9	
Time on source (hr)	3.0	
Rest frequency (GHz)	36.16929	
Target source velocity (km/s)	39.8	
Hanning smoothing	No	
Beam Size (arcsec x arcsec)	0.48 x 0.18	
Line rms noise (mJy/beam)	10.0	

[a] The units of Right Ascension (R.A.) are in (hour, minutes, seconds), whereas the units of Declination are in (degrees, arcminutes, arcseconds).

3. Results

Figure 2 shows an image of the Sagittarius A supernova remnant from Sjouwerman et al. (2010). They observed ten Class I methanol masers in this supernova remnant (at 36 GHz), and the locations of these masers are marked in the figure by plus signs. Of these, the two strongest Class I methanol masers (GCMM1 and GCMM4) were targeted for the Zeeman effect observations described in this thesis. Figure 3 shows an image of one of these masers (GCMM 1) from the VLA observations reported in this thesis. The image shown is for the spectral channel in which the maser has its peak intensity of 326.1 Jy/beam. The maser is clearly unresolved, as is evident by comparing with the beam displayed in the lower left corner. However, there is no other maser in that channel within 6.65 arcseconds.

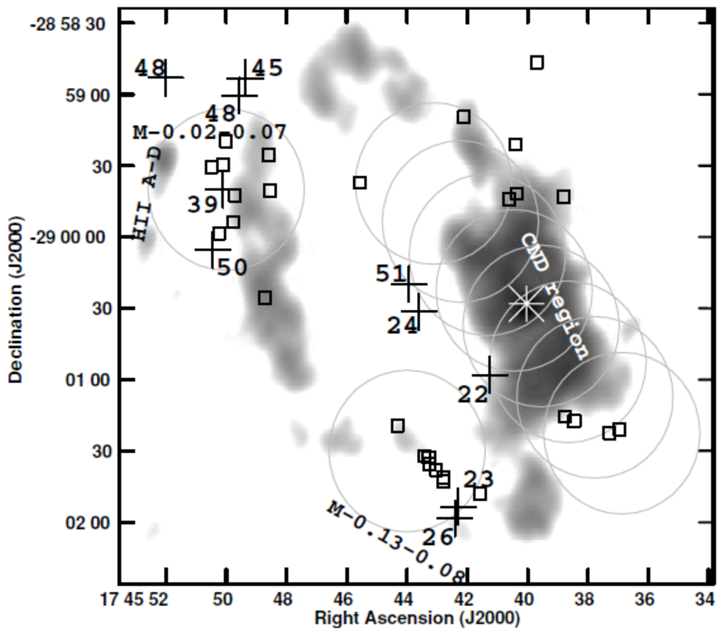

Figure 2. Image from Sjouwerman et al. (2010) showing the location of ten 36 GHz methanol masers in the Sagittarius A supernova remnant. The maser locations are indicated by plus signs. The masers chosen for this study were the two with the highest intensity, which we have designated as GCMM1 and GCMM4. The former is labeled as number 39 in the figure above, whereas GCMM4 does not correspond to any of the positions listed above, but is nearest to number 26. The circles show the 68″ diameter primary beams employed in different pointings by Sjouwerman et al. (2010) to cover as much of the extended source structure of the supernova remnant as possible (although note that they report in their paper that they have included structures up to 2.5 times beyond their primary beam).

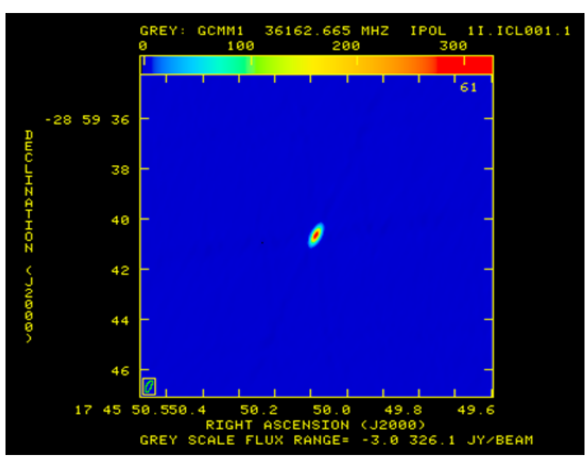

Figure 3. Image of the maser GCMM1 in its peak spectral channel from the observations reported in this thesis. The maser is in the supernova remnant Sagittarius A toward the Galactic Center. The peak value of the maser in this spectral channel is 326.1 Jy/beam.

Figure 4 and Figure 5 show the Stokes *I* and *V* spectral line profiles for the masers GCMM1 and GCMM4, respectively, from our VLA observations. As described in Section 2, the Stokes *I* profile gives the total intensity of the maser, and the Stokes *V* profile is the difference of the right and left circularly polarized signals received at the telescope. The yellow histogram-like Stokes *I* profile in the upper panel of each figure shows the observed intensity of the maser. The vertical axis in the upper panel gives the intensity of the maser in Jy/beam. Spectra in physics are usually plotted against frequency on the horizontal axis, but radio astronomers display velocities along the horizontal axis, where the velocities are calculated by measuring the frequency offsets from the rest frequency of the spectral line. Both profiles (in Fig. 4 and 5) suggest the presence of several maser components in velocity space. Therefore, we used the AIPS task ZEMAN to fit four Gaussian components each to the Stokes *I* profiles of GCMM1 and GCMM4; these are shown in light blue in the upper panel, and the resultant profile in green is overlaid on the observed histogram-like Stokes I profile. To fit the Stokes *I* profile of GCMM1, we needed one strong and broad profile with an intensity of 200 Jy/beam and a velocity width of 1.25 km/s (the so-called full width at half the maximum intensity, or FWHM), one relatively strong narrow profile with intensity of 125 Jy/beam and a velocity width of 0.25 km/s, and two lower intensity profiles of ~40 Jy/beam with FWHM velocity widths of ~0.4 km/s each. To fit the Stokes *I* profile of GCMM4, we needed one strong and narrow profile with an intensity of 63 Jy/beam and a FWHM velocity width of ~0.5 km/s, and three low intensity and broad profiles with intensities of 5, 8, and 10 Jy/beam respectively and FWHM velocity widths of ~0.8 km/s. The histogram-like lines in the lower panels of Figure 4 and Figure 5 show the observed Stokes *V* profiles. As noted above, the Stokes *V* profile is obtained by subtracting the left circularly polarized signal from the right circularly polarized signal, where right circular polarization is defined as the clockwise rotation of the electric vector when viewed along the direction of wave propagation.

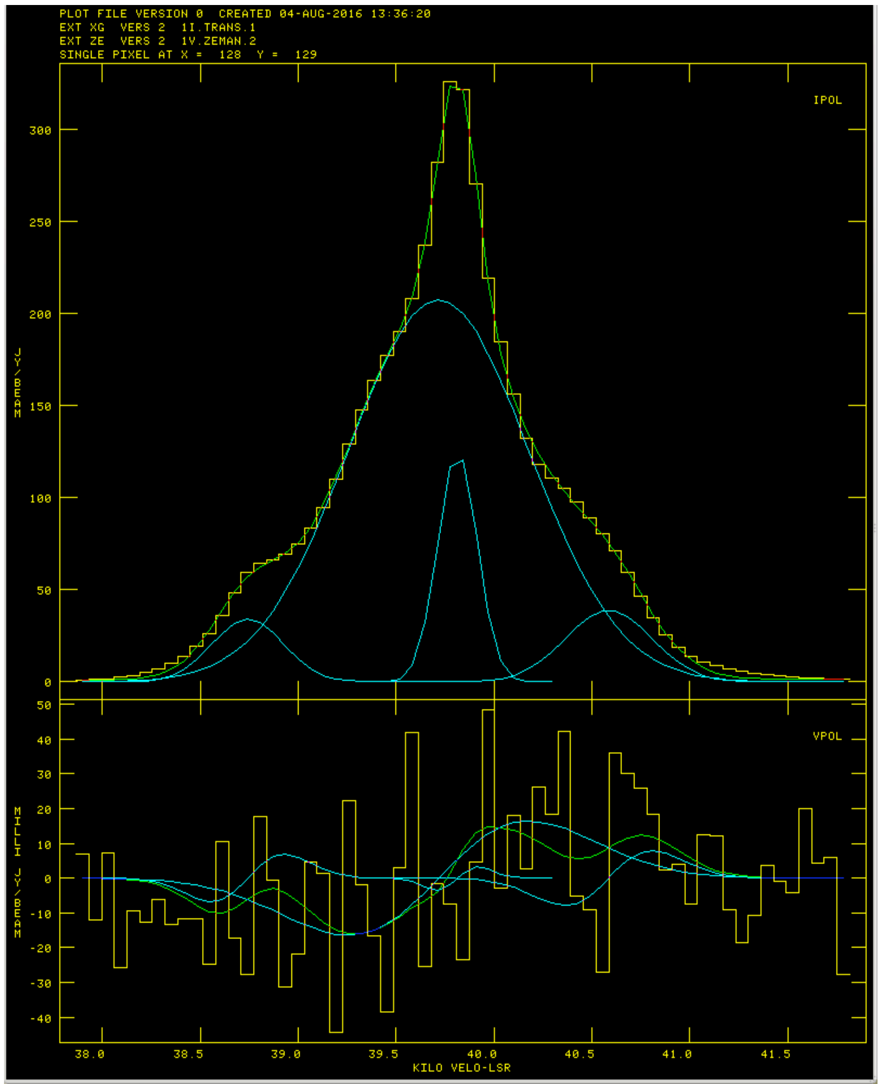

Figure 4. Observed Stokes *I* (top histogram-like line) and Stokes *V* (bottom histogram-like line) profiles for the maser GCMM1. The blue-colored profiles in the upper panel show the four Gaussian components that were fit to the Stokes *I* profile, and the green curve is the resultant sum of these four Gaussians. The derivatives of each of these profiles, scaled by the fitted value of *b* (see equation 1 and Table 2), are shown in the lower panel by the blue curves, and the green curve is the resultant sum of these four; it may not be visible in some places because the strongest blue component overlays it.

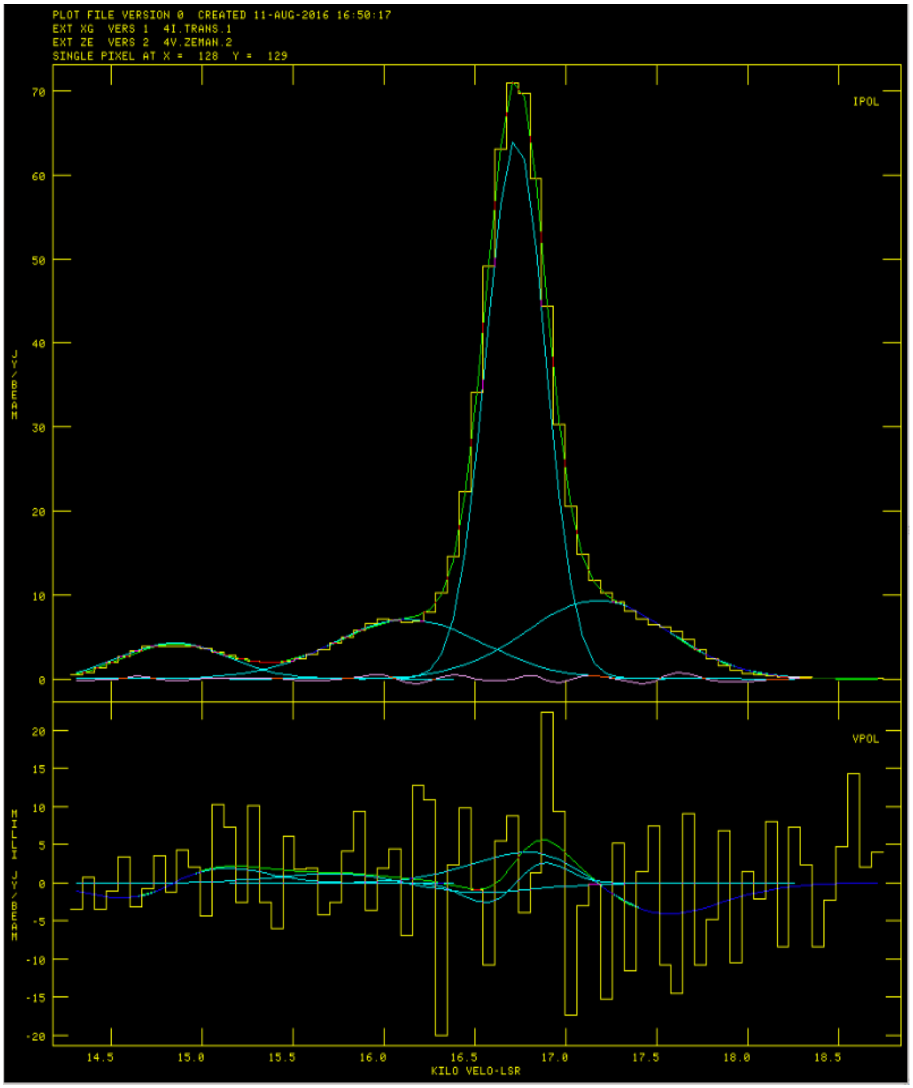

Figure 5. Observed Stokes *I* (top histogram-like line) and Stokes *V* (bottom histogram-like line) profiles for the maser GCMM4. In the upper panel the blue profiles show the four Gaussian components that were fit to the Stokes *I* profile, and the green curve is the resultant sum of these four Gaussians. The blue curves in the lower panel show the derivatives of each of these profiles, scaled by the fitted value of *b* (see equation 1 and Table 2), and the green curve is the resultant sum of these four although it is not visible in some areas as the strongest blue curve overlays it.

If a Zeeman effect is present, then the observed Stokes *V* profile should look like the derivative of the Stokes *I* profile. However, small leaks in the signal recorded at the receivers usually result in a scaled-down replica of the Stokes *I* profile in the Stokes *V* profile. In practice, therefore, observers usually fit the observed Stokes *V* profile simultaneously to a scaled-down replica of the Stokes *I* profile and its derivative, by doing

$$V = aI + \frac{b}{2}\frac{dI}{d\nu} \tag{1}$$

The parameter "*a*" in this fit is a small number ($\sim 10^{-3}$) that represents the presence of a scaled-down replica of the Stokes *I* profile in the *V* profile, and the parameter "*b*" is a product of the Zeeman splitting factor for the observed line (in this case, methanol), times the line-of-sight magnetic field in the maser region, so that

$$b = zB_{\text{los}} \tag{2}$$

The AIPS task ZEMAN allows for the four Gaussian components in the Stokes *I* profile to be fitted by different values of "*b*" to match the observed Stokes *V* profile. Each value of "*b*" would then correspond to a different value of the line of sight magnetic field. The fitted values of "*b*" for each of the four components of GCMM1 and GCMM4 are shown in Table 2, along with the 1-sigma error from these fits. We have left the values in terms of "*b*" because the Zeeman splitting factor *z* for methanol has never been measured.

Table2. Fitted values of "*b*" for our observed masers

Gaussian component number	*b for* GCMM1 (Hz)	*b for* GCMM4 (Hz)
1	14.56±5.60	2.65±3.42
2	14.61±19.79	-28.27±61.87
3	1.11±4.02	52.90±69.10
4	17.72±19.44	-67.42±44.92

Note: The parameter $b = zB_{\text{los}}$, where z is the Zeeman splitting factor (in Hz/mG), and B_{los} is the line of sight magnetic field (in mG). The value of *z* for methanol masers is unknown, and so the results are reported as *b* (in Hz).

4. Discussion and Analysis

From the fitted values of "*b*" given in Table 2, it is clear that none of the four Stokes *V* components for either the GCMM1 or GCMM4 masers offers a detection of the Zeeman effect that is at a 3-sigma or greater level in the spectra. Observers will not claim that they have detected a Zeeman effect unless they have such a 3-sigma result, or a higher level of significance. This is also clear from a visual examination of the Stokes *V* profiles in Figure 4 and Figure 5, where most lie at or below the noise level. By contrast, consider the detection of the Zeeman effect in the Class I methanol maser line toward the star forming region OMC-2 from Momjian and Sarma (2012), shown in Figure 6. They fitted their observed Stokes *V* profile with $b = 18.4$ Hz. The *S*-shaped aspect of their Stokes *V* profile, well above the noise level in the profile, is clearly seen in Figure 6.

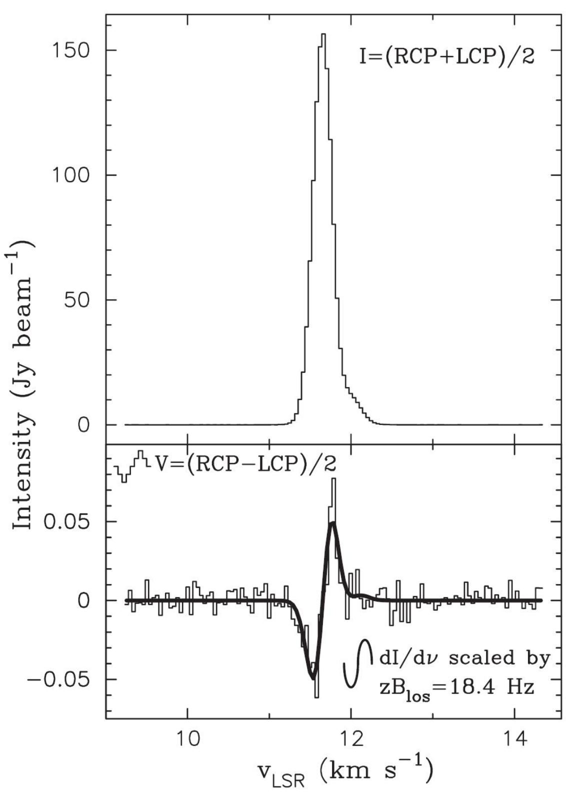

Figure 6. Stokes I and V profiles from a 44 GHz class I methanol maser toward a star forming region in OMC-2 from Momjian & Sarma (2012).

The best result from our VLA observations is in the 39.7 km/s component toward GCMM1, for which there is a 2.6-sigma result. For the rest, the results are closer to 1-sigma. One reason for this non-detection could be that the magnetic field at the location of both masers (GCMM1 and GCMM4) lies primarily in the plane of the sky, so that its line of sight component is tiny. Another possibility is that the line of sight magnetic field reverses direction on very small scales. If the maser components were well separated in velocity space, this would not be much of an issue, but since they are closely spaced together in velocity, such reversals could cancel, leaving a zero net magnetic field on the aggregate. From Figure 4 and Figure 5, it is clear that maser lines are tangled in velocity space. Untangling the fields traced by these components would be extremely difficult unless there is one component that is exceptionally strong as to remain not canceled or the field is uniform throughout and does not exhibit reversals on small scales. Neither appears to be the case for the two sources observed in this thesis. Nevertheless, our observations do place some constraint on the fields. The 1-sigma upper limit on the fields for GCMM1 is 37Hz and for GCMM4 is 112 Hz. This would be in line with other discoveries, e.g., Momjian and Sarma (2009) found magnetic field *b* values of -53.2 ± 6.0 Hz and 34.4 ± 5.9 Hz within a 36 GHz class I methanol maser.

5. Conclusion

Supernovae are the end stages of high mass stars, stars with masses about eight times that of the Sun or greater. Left behind after such a supernova is a shell of matter surrounding the former position of the star that is known as a supernova remnant. Material in supernova remnants enriches the gas from which a subsequent generation of stars will be formed. Much remains unanswered about the early stages of star formation, especially high mass star formation. In particular, we know that magnetic fields play an important role in the star formation process, and so it is important to measure them in as many different environments as is possible. The Zeeman effect in Class I methanol masers offers the possibility of measuring magnetic fields in several astrophysical environments. Class I methanol masers are formed by collisional processes and have been discovered in supernova remnants. We would like to measure magnetic fields in these remnants since their material will enrich the next generation of stars. We observed two maser sources (GCMM1 and GCMM4) in the supernova remnant Sagittarius A toward the Galactic Center with the VLA radio telescope array. The observed total intensity (Stokes *I*) profiles for these masers sources are complex, and had to be fitted with four Gaussian components. Fits to the observed Stokes *V* profiles of these masers have yielded only upper limits on the magnetic field, with the best case being a 2.6-sigma detection in the 39.7 km/s of the maser source GCMM1. This is not surprising, since the four fitted Gaussian components are closely blended in velocity for both maser sources. Either the magnetic field in both sources is largely in the plane of the sky so that its line of sight component is small, or the field reverses on very small scales so that it cancels out in summing over the four components. Future observations would be successful in detecting magnetic fields if maser sources exist that have simpler profiles, or if environments exist in which the field is overwhelmingly large in one component.

References

Elmegreen, Bruce G. (1978) "On the Determination of Magnetic Fields in Dense Cloud Complexes by the Observation of Zeeman Splitting," *The Astrophysical Journal Letters*: 225:L85-L88

Federrath, C.; Rathborne, J. M.; Longmore, S. N.; Kruijssen, J. M. D.; Bally, J.; Contreras, Y.; Crocker, R. M.; Garay, G.; Jackson, J. M.; Testi, L.; Walsh, A. J. (2016) "The Link between Turbulence, Magnetic Fields, Filaments, and Star Formation in the Central Molecular Zone Cloud G0.253+0.016," *The Astrophysical Journal*, Volume 832, Issue 2, article id. 143, 18 pp.

Kamitsukasa, Fumiyoshi; Koyama, Katsuji; Nakajima, Hiroshi; Hayashida, Kiyoshi; Mori, Koji; Katsuda, Satoru; Uchida, Hiroyuki; Tsunemi, Hiroshi (2016) "Suzaku study on the ejecta of the supernova remnant G272.2-3.2," *Publications of the Astronomical Society of Japan*, Volume 68, Issue SP1, id.S7 9 pp.

McMullin, J. P.; Golap, K.; Myers, S. T. (2004) "The AIPS++ Project," *ASP Conference Series*: Vol. 314,

Moran, J. M.; (1990) "Magnetic fields in interstellar masers," *Galactic and intergalactic magnetic fields*; Proceedings of the 140th Symposium of IAU, Heidelberg, Federal Republic of Germany, June 19-23, 1989 (A91-46626 20-90). Dordrecht, Netherlands, Kluwer Academic Publishers, 1990, p. 301-303.

Myers, P. C.; Goodman, A. A. (1995) "Observations of Magnetic Fields in Diffuse Clouds," *The Astrophysical Journal Letters*: 442:177-185

Sarma, Anuj P.; Momjian, Emmanuel (2009) "Detection of the Zeeman Effect in the 36 GHz Class I CH3OH Maser Line with the EVLA," *The Astrophysical Journal*: 705:L176–L179

Sjouwerman, Lorant; Pihlstrom, Ylva M.; Fish, Vincent L. (2010) "Expanded Very Large Array Detection of 36.2 GHz Class I Methanol Masers in Sagittarius A," *The Astrophysical Journal Letters*: 710:L111–L114

Williams, Brian. "What is a supernova Remnant?" NCSU.edu